Available online at www.ijpe-online.com

International Journal of Performability Engineering

Vol. 13, No. 7, November 2017, pp. 1140-1146
DOI: 10.23940/ijpe.17.07.p17.11401146

Speed Control Simulation of the Electric Vehicle Driving Motor

Wanmin Li[a,b,*], Menglu Gu[b], Lulu Wei[b]

[a]*School of Automobile Engineering, Lanzhou Institute of Technology, Lanzhou 730050, China*
[b]*School of Automobile, Chang'an University, Xi'an 710064, China*

Abstract

In order to realize precise speed control of driving motor, an adaptive fuzzy PID control strategy for motors was established based on the existing proportional–integral–derivative (PID) control theory. The motor speed control model is built by simplifying the parameters of a brushless DC motor using the Sim Power Systems toolbox in MATLAB/Simulink environment, which involves the simulation of motor speed control including low speed, high speed, and road bump situations in city traffic environment. Results show that the time of the adaptive fuzzy PID control is 0.08s at low speed, the adjustment time of the conventional PID control is 0.22s, and the adjustment times are 0.12s and 0.32s at high speed. After encountering road bumps, the adaptive fuzzy PID control can quickly react and return to normal speed, whereas the conventional PID control is evidently affected by the interference.

Keywords: fuzzy Control; PID control; simulation; electric vehicle

(Submitted on August 31, 2017; Revised on October 5, 2017; Accepted on October 23, 2017)

1. Introduction

New energy vehicles, particularly hybrid and pure electric vehicles, are currently developing at a rapid rate. Research on the precise control of automotive drive motors is becoming increasingly important. A growing number of existing motor drive vehicles are using permanent magnet brushless DC motors inconsideration of motor torque, power density, and cost factors [1]. However, such motors exhibit strong coupling and nonlinear characteristics, whereas traditional studies on motor control use the proportional–integral–derivative (PID) control [2], which has a simple structure that can satisfy certain robustness requirements for common applications in the industrial field [3]. However, as a power source for vehicles, the precision of PID control cannot satisfy the demands of drivers for control and comfort [4].

The typical results of current local and international research on motor control exhibit disadvantages, including the low precision of the traditional PID control [5]. Several scholars adopted the fuzzy control algorithm to solve the aforementioned problems. However, fuzzy control must be built based on a certain amount of historical data and an empirical attribute is important in selecting a fuzzy membership function [6]. Similar to the use of the fuzzy control method, some engineers introduced a neural network into brushless DC motor rotation control and designed a control system with a digital signal processor as the control unit [7,10]. In summary, although research results on motor control are abundant, studies on the applications of such motors to vehicles and on the precise control of vehicles based on the requirements of drivers for driving and riding comfort remain lacking [8]. In the current work, a brushless DC driving motor is selected as the object of study. Then, a motor control method based on fuzzy control and adaptive PID control is proposed to optimize motor control accuracy [9].

2. Mathematical Model of Motor

A permanent magnet brushless DC motor has a trapezoidal back electromotive force (EMF) and a rectangular current wave form. The mutual inductance produced by the rotor and the stator is nonlinear [10]. It is frequently simplified in research by assuming the following: In absence of the alveolar effect, the windings are evenly distributed inside the stator, armature

* Corresponding author.
E-mail address: 308510520@qq.com.

reaction is disregarded, the winding symmetry has three phases, and losses due to hysteresis and eddy currents are not considered. The voltage balance equation for the motor winding is simplified as follows:

$$\begin{bmatrix} u_a \\ u_b \\ u_c \end{bmatrix} = \begin{bmatrix} r & 0 & 0 \\ 0 & r & 0 \\ 0 & 0 & r \end{bmatrix} \begin{bmatrix} i_a \\ i_b \\ i_c \end{bmatrix} + \begin{bmatrix} L & M & M \\ M & L & M \\ M & M & L \end{bmatrix} p \begin{bmatrix} i_a \\ i_b \\ i_c \end{bmatrix} + \begin{bmatrix} e_a \\ e_b \\ e_c \end{bmatrix} \tag{1}$$

where the winding voltage of the stator is denoted as u_a, u_b, u_c; the winding electric current of the stator is denoted as i_a, i_b, i_c; the winding EMF of the stator is denoted as e_a, e_b, e_c; and the inductance of each phase winding, the mutual inductance between the arbitrary two-phase windings, and the differential operators are respectively denoted as *L*, *M*, and *p*. The resulting phases obtain a trapezoidal back EMF and are rectangular current waveform, as shown in Figure 1.

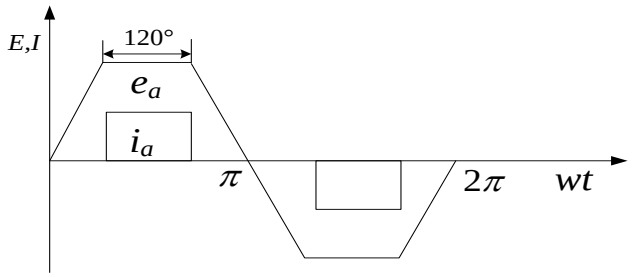

Figure 1. Phase current and back EMF

When the brushless DC motor is considered, no central line is observed among the three windings, i.e.,

$$i_a + i_b + i_c = 0 \tag{2}$$

$$Mi_a + Mi_b + Mi_c = 0 \tag{3}$$

Therefore, the voltage balance equation for the new motor winding is obtained as follows:

$$\begin{bmatrix} u_a \\ u_b \\ u_c \end{bmatrix} = \begin{bmatrix} r & 0 & 0 \\ 0 & r & 0 \\ 0 & 0 & r \end{bmatrix} \begin{bmatrix} i_a \\ i_b \\ i_c \end{bmatrix} + \begin{bmatrix} L & 0 & 0 \\ 0 & L & 0 \\ 0 & 0 & L \end{bmatrix} p \begin{bmatrix} i_a \\ i_b \\ i_c \end{bmatrix} + \begin{bmatrix} e_a \\ e_b \\ e_c \end{bmatrix} \tag{4}$$

The motor circuit represented by the upper type may be equivalent to Figure 2.

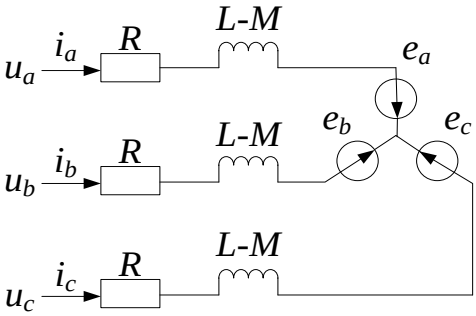

Figure 2. Equivalent motor circuit

Furthermore, the torque and motion equations for the simplified brushless DC motor are as follows:

$$T_e = \frac{e_a i_a + e_b i_b + e_c i_c}{w} \tag{5}$$

$$T_e - T_L = J\frac{\mathrm{d}w}{\mathrm{d}t} + Bw \tag{6}$$

Where the motor electromagnetic torque is denoted as T_e, the rotor angular velocity is denoted as w, the load torque is denoted as T_l, and the motor self-rotating inertia is denoted as J.

3. Double closed-loop control system based on fuzzy PID method

3.1. System structure

The motor adopts the double closed-loop control strategy for rotation speed and phase current. The main and auxiliary rings control rotation speed and phase current, respectively. The ideal motor control process is the vehicle reaching the maximum at the starting stage to generate maximum acceleration. The drive current drops rapidly when vehicle speed accelerates to table stage, which balances the force and load of the driving motor. The phase current cannot be rapidly reduced because of the presence of inductance in the motor, and a certain amount of time is required to start the vehicle rapidly within acceptable limits after the current reaches its maximum value [11]. Therefore, the double loop control strategy for rotation speed and phase current is introduced into the motor control. The motor control process is illustrated in Figure 3.

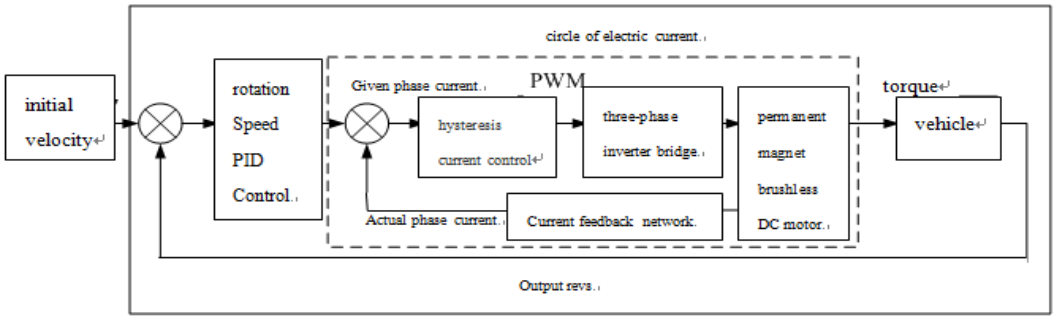

Figure 3. Flowchart of motor control procedure

3.2. Design of adaptive fuzzy PID control

The fuzzy PID control consists of two parts: fuzzy control and PID control. To receive rapid and correct responses after system inputs, model error e and error change rate e_c are continually detected while the system is operating. Then, in accordance with the fuzzy control rule, the PID control parameters k_p, k_i, k_d are correspondingly regulated based on their relations to enable model error e and error change rate e_c to satisfy all system requirements. The structure of the fuzzy PID controller is shown in Figure 4. In the figure, model error e and error change rate e_c are obtained after comparing system inputs and outputs. To fulfill the requirements of fuzzy fields, a quantization factor is adopted to magnify or diminish the signal to an appropriate extent, which is then regarded as the final input of the fuzzy control system. The fuzzy controller calculates the correction of the PID adjustable parameter based on the scaling parameter. Through this process, new control parameters, namely, k_p, k_i, k_d , are obtained by the PID controller, which are then applied to the controlled target.

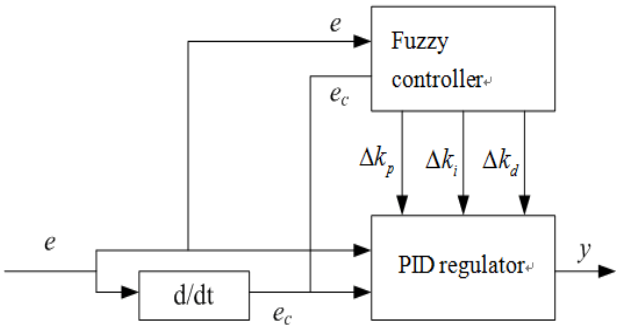

Figure 4. Flowchart of fuzzy PID control

Three fuzzy controllers are adopted in this study. Model error e and error change rate e_c are used as the inputs of each controller. Three adjustable parameters are used as the output sin PID control; that is, a double-input single-output method is implemented. In accordance with actual demands, this study considers *Mandani* and designs a fuzzy inference system (FIS)

control bin using MATLAB. The fuzzy domain is set to [−6, 6]. The fuzzy subsets of each controller are all set to {NB, NM, NS, ZO, PS, PM, and PB}.The subsets represent *negative big*, *negative middle*, *negative small*, *zero*, *plus small*, *plus middle*, and *plus big*. The triangle membership function is selected with high sensitivity and resolution to acquire good robustness and practicability of the fuzzy controller. The membership functions of the fuzzy controller are defined in Figure 5.

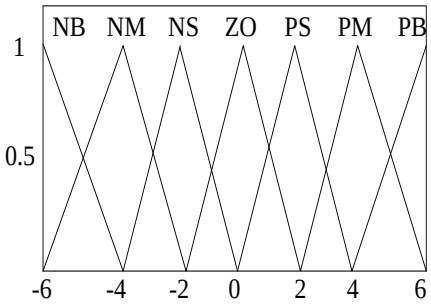

Figure 5. Membership functions of fuzzy controller

The establishment of fuzzy control rules, which is realized mostly through the experience of experts or the statistical induction of historical data, is an important aspect of fuzzy control. The correction factors of PID parameters are obtained by considering tuning, as shown below:

Table 1. $\triangle k_p$ Fuzzy rules

e	e_c						
	NB	NM	NS	ZO	PS	PM	PB
NB	PB	PB	PM	PM	PS	ZO	ZO
NM	PB	PB	PM	PS	PS	ZO	NS
NS	PM	PM	PM	PS	ZO	NS	NS
ZO	PM	PM	PS	ZO	NS	NM	NM
PS	PS	PS	ZO	NS	NS	NM	NM
PM	PS	ZO	NS	NM	NM	NM	NB
PB	ZO	ZO	NM	NM	NM	NB	NB

Table 2. $\triangle k_i$ Fuzzy rules

e	e_c						
	NB	NM	NS	ZO	PS	PM	PB
NB	NB	NB	NM	NM	NS	ZO	ZO
NM	NB	NB	NM	NS	NS	ZO	ZO
NS	NM	NM	NS	NS	ZO	PS	PS
ZO	NM	NM	NS	ZO	PS	PM	PS
PS	NM	NS	ZO	PS	PS	PM	PB
PM	ZO	ZO	PS	PS	PM	PB	PB
PB	ZO	ZO	PS	PM	PM	PB	PB

Table 3. $\triangle k_d$ Fuzzy rules

e	e_c						
	NB	NM	NS	ZO	PS	PM	PB
NB	PS	NS	NB	NB	NB	NM	PS
NM	PS	NS	NB	NM	NM	NS	ZO
NS	ZO	NS	NM	NM	NS	NS	ZO
ZO	ZO	NS	NS	NS	NS	NS	ZO
PS	ZO	ZO	ZO	ZO	ZO	ZO	ZO
PM	PB	PS	PS	PS	PS	PS	PB
PB	PB	PM	PM	PM	PS	PS	PB

The outputs of adopting fuzzy control rules are several fuzzy sets. However, precise inputs are required to control the motor, and thus, the fuzzy control consequence should be clear. Existing methods for achieving clearness include the average area method, the maximum membership degree method, and the center-of-gravity method. In this study, the simple center-of-gravity method is used to conduct clearness processing. The modified control parameters are derived by substituting the control variables {e, e_c}p obtained from the fuzzy control into the above equations and combining the quantization factor of the fuzzy control. The final fuzzy PID control output can be acquired after the modified parameters are added to the initial control parameters.

$$k_p = k_{p0} + k_{u1}\{e, e_c\}p \tag{7}$$

$$k_i = k_{i0} + k_{u2}\{e, e_c\}i \tag{8}$$

$$k_d = k_{d0} + k_{u3}\{e, e_c\}d \tag{9}$$

In the last equation, k_{p0}, k_{i0}, k_{d0} represent the initial control parameters, whereas k_{u1}, k_{u2}, k_{u3} are the fuzzy controller quantization factors. The initial control parameters are determined by trial and error, and a conventional PID control model for a brushless DC motor is established beforehand. The parameters are constantly adjusted, and the influence of such adjustment is analyzed. Then, the PID parameters are selected, which provides a steady and acceptable overshoot result as the initial input value of the fuzzy PID control. The initial PID control parameters that are adopted after the first tuning are 3, 0.15, and 0.02.

3.3. Establishment of fuzzy PID control model

The workload for independently developing and establishing a motor control model is heavy. A module library is integrated into the Simulink platform of MATLAB to be used for the motor control model. This procedure provides convenience for motor modeling and control, such as the insulated gate bipolar transistor module, which is necessary for establishing an inverter. In this study, the model for the fuzzy PID control is built using the Sim Power System toolbox, as shown in Figure 6.

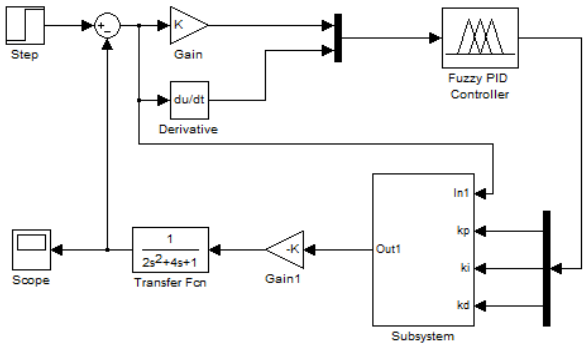

Figure 6. Block diagram of fuzzy PID control

4. Model simulation and analysis

The established model is tested in Simulink environment, and the sampling time T of the simulation system is set to 0.0005s. A common type of vehicle-driving brushless DC motor is used as the motor prototype, and its basic parameters are as follows: winding inductance *L* is 0.02H, mutual inductance Mis−0.067H, damping coefficient *B* is 0.0002, total resistance *R* is 1Ω, rotary inertia of the motor rotor *J* is 0.005kg•m2, pole log *P* is 1, back EMF coefficient ke is 0.382, and motor voltage rating *U* is standard at 220V. On the basis of the aforementioned settings, the PID control initial parameters, including the quantification factor and the proportion factors k_e, k_{u1}, k_{u2}, and k_{u3}, are set to 0.01, 0.38, 0.01, and 0.01, respectively. The vehicle parameters mainly consider the components at the lower end of the motor output and the basic parameters of the vehicle under running condition. It includes the minimum running speed; atypical urban road is selected as an example. The minimum speed is 30km/h, the maximum speed is 80km/h, the rolling radius of the vehicle driving wheel is 0.367m, and the transmission ratio is 1. In accordance with the relationship between vehicle speed and motor speed

$$u_a = 0.377\frac{rn}{i_g i_o} \tag{10}$$

The low and high motor speed are approximately 220r/min and 580r/min, respectively. The aforementioned initial state is inputted to obtain the simulation results at low and high speeds, as shown in Figures 7 and 8. From the simulation results, the target speed for low speeds is 220r/min. The time required for system tuning is approximately 0.2s for the conventional non-adaptive fuzzy PID control system. Although the reaction time is longer, no overshoot phenomenon occurs. The regulation time of the model proposed in this study is only 0.08s. Response becomes faster at the same speed and no overshoot occurs. The target speed for high speeds is 580r/min. Furthermore, the required system tuning time is approximately 0.32s for the conventional fuzzy PID control system. Correspondingly, the regulation time is only 0.12s when the self-adaptive fuzzy PID control system proposed in this study is adopted. The differences between the two systems are apparent in terms of reaction time. On the basis of the reaction time required by the system, time is extremely short and basically fulfills the requirements of system response time.

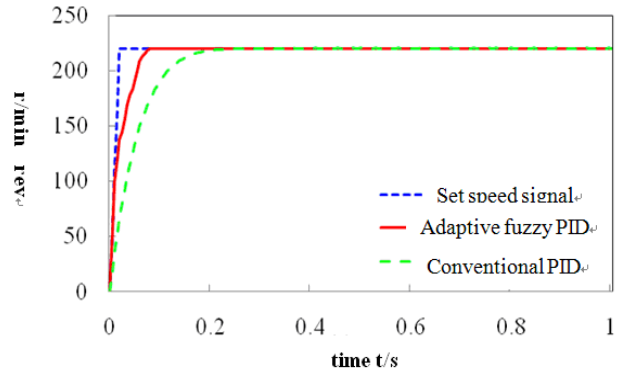

Figure 7. Simulation results at low speed

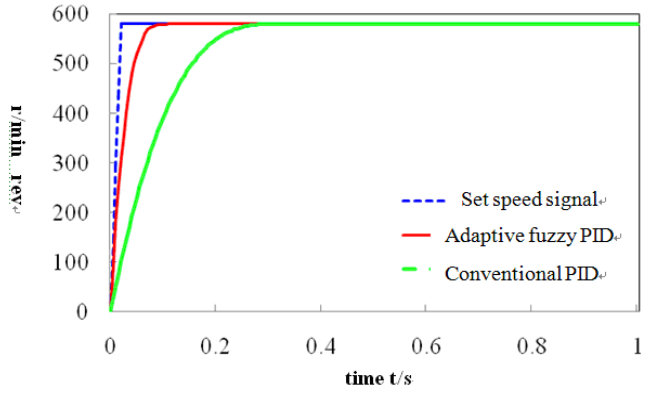

Figure 8. Simulation results at high speed

In the normal driving process, particularly in a low-speed case, the vehicle is subjected to bumps on the road surface. Therefore, when brushless DC motor speed control experiments are performed, the conditions of the road where the vehicle is traveling must be considered. In the simulation process, a certain interference load is applied to the motor, and the load is added at 0.4-0.6s. Then, the different effects of the conventional PID control system and the self-adaptive fuzzy PID control system are analyzed. The results are presented in Figure 9. As shown in the figure, motor speed is reduced significantly after the load is added. The effect of the conventional PID control is not apparent and motor speed is in a disturbed state. In contrast, the effect of the adaptive fuzzy PID control is evident. The adaptive fuzzy PID control can react quickly and return to normal speed, whereas the conventional PID control is affected considerably by interference. The adaptive fuzzy PID control exhibits strong adaptability.

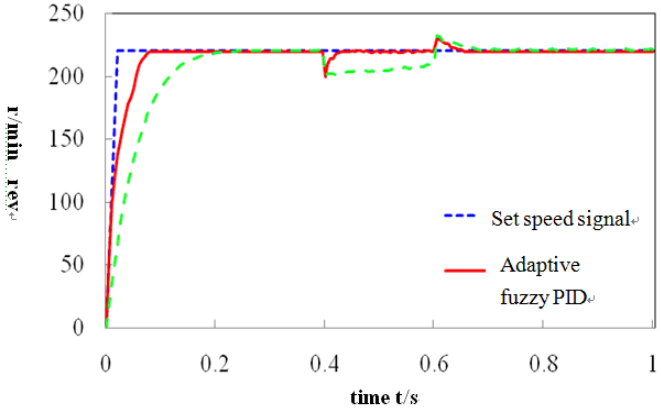

Figure 9. Simulation results under load application

5. **Conclusions**

The mature PID control strategy is adopted and combined with an existing optimized fuzzy control that is commonly used in the control field to realize precise control of the speed of a driving motor. An adaptive fuzzy PID control strategy for

brushless DC motors is established and the motor speed control model is built in MATLAB/Simulink environment. Simulation test are performed and the following conclusions are drawn.

In low-speed case, the adaptive fuzzy PID control adjustment time is 0.08s, whereas the conventional PID control adjustment time is 0.22s. In a high-speed case, the adaptive fuzzy PID control adjustment time is 0.12s, whereas the conventional PID control adjustment time is 0.32s. Accordingly, the adaptive fuzzy PID control is more adaptable than the conventional PID control.

An interference load is added to the simulation to consider the bumps caused by road roughness while traveling. The results show that the adaptive fuzzy PID control can react rapidly and return to normal speed, whereas the conventional PID control is evidently affected by such interference.

Acknowledgements

This work was partly financially supported through grants from Scientific Research Project of Universities in Gansu Province (2017A-110) and Young Science and Technology Innovation Project of Lanzhou Institute of Technology(16K-004).

References

1. L. Breiman, “Random Forests”, *Machine Learning*, vol. 45, no. 1, pp. 5-32, 2001
2. A. Choudhury, P. Pillay, “DC-Link Voltage Balancing for a Three-Level Electric Vehicle Traction Inverter Using an Innovative Switching Sequence Control Scheme”, *IEEE Journal of Emerging and Selected Topics in Power Electronics*, vol. 2, no. 2, pp. 296-307, 2014
3. B. Hamed, M. Almobaied, “Fuzzy PID Controllers Using FPGA Technique for Real Time DC Motor Speed Control”, *Intelligent Control and Automation*, vol. 2, no. 3, pp. 233-240, 2011
4. J. J. Justo, F. Mwasilu, “Fuzzy Model Predictive Direct Torque Control of IPMSMs for Electric Vehicle Applications,” *IEEE/ASME Transactions on Mechatronics*, vol. 22, no. 4, pp. 1542-1553, 2017
5. M. Jalali, A. Khajepour, “Integrated stability and traction control for electric vehicles using model predictive control”, *Control Engineering Practice*, vol. 54, no. 9, pp. 256-266, 2016
6. M. Muruganandam, M. Madheswaran, “Experimental verification of chopper fed DC series motor with ANN controller”, *Frontiers of Electrical and Electronic Engineering*, vol. 7, no. 4, pp. 477-489, 2012
7. S. D. Pinto, P. Camocardi, “Torque-Fill Control and Energy Management for a Four-Wheel-Drive Electric Vehicle Layout with Two-Speed Transmissions,” *IEEE Transactions on Industry Applications*, vol. 53, no. 1, pp.447–458, 2016
8. R. Shi, S. Semsar, “Constant Current Fast Charging of Electric Vehicles via a DC Grid Using a Dual-Inverter Drive”, *IEEE Transactions on Industrial Electronics*, vol. 64, no. 9, pp. 6940-6949, 2017
9. X. Shi, M. Krishnamurthy, “Survivable Operation of Induction Machine Drives with Smooth Transition Strategy for EV Applications”, *IEEE Journal of Emerging and Selected Topics in Power Electronics*, vol. 2, no. 3, pp. 609-617, 2014
10. P. Walker, B. Zhu, “Powertrain dynamics and control of a two speed dual clutch transmission for electric vehicles,” *Mechanical Systems and Signal Processing*, vol. 85, no. 2, pp. 1-15, 2017.
11. Z. Yang, F. Shang, “Comparative Study of Interior Permanent Magnet, Induction, and Switched Reluctance Motor Drives for EV and HEV Applications”, *IEEE Transactions on Transportation Electrification*, vol. 1, no. 3, pp. 245-254, 2015